Tolerance optimization by modification of Taguchi's robust design approach and considering performance levels

Manuel Paredes, Romain Canivenc, Marc Sartor

▶ **To cite this version:**

Manuel Paredes, Romain Canivenc, Marc Sartor. Tolerance optimization by modification of Taguchi's robust design approach and considering performance levels: Application to the design of a cold-expanded bushing. Proceedings of the Institution of Mechanical Engineers, Part G: Journal of Aerospace Engineering, 2014, 228 (8), pp.1314–1323. hal-01952587

HAL Id: hal-01952587

https://ut3-toulouseinp.hal.science/hal-01952587

Submitted on 2 Aug 2022

HAL is a multi-disciplinary open access archive for the deposit and dissemination of scientific research documents, whether they are published or not. The documents may come from teaching and research institutions in France or abroad, or from public or private research centers.

L'archive ouverte pluridisciplinaire **HAL**, est destinée au dépôt et à la diffusion de documents scientifiques de niveau recherche, publiés ou non, émanant des établissements d'enseignement et de recherche français ou étrangers, des laboratoires publics ou privés.

Tolerance optimization by modification of Taguchi's Robust Design approach and considering performance levels. Application to the design of a cold-expanded bushing

http://dx.doi.org/10.1177/0954410013489953

M. Paredes, R. Canivenc, M. Sartor

Université de Toulouse; INSA, UPS, Mines Albi, ISAE; ICA (Institut Clément Ader); 135, avenue de Rangueil, F-31077 Toulouse, France

manuel.paredes@insa-toulouse.fr

Tel. +33 5 61 55 99 56

Abstract

This paper defines a method for the optimization of design parameter tolerances. The general architecture of the proposed method is identical to that of the robust design reference method proposed by Taguchi but its content is different as the tolerances are considered as functions to be maximized here, while Taguchi's method rather considers these tolerances as fixed data. Instead of looking for design parameters that minimize the sensitivity of some performance criteria, the design parameters are calculated so as to obtain maximal tolerance intervals, thus minimizing manufacturing costs. Performance criteria are then considered in terms of

optimization constraints: each criterion gives rise to an inequality constraint that specifies the minimum level of performance that the designer wants to achieve. The possibilities offered by this method are illustrated through its use in the preliminary design of a cold-expanded bushing. In this case, tolerance optimization enables the allowable tolerances on the design diameters to be increased and performance levels are defined on the residual radial stress at the bushing/part contact radius and on the residual orthoradial (hoop) stress at the part inner radius.

Keywords

Tolerance optimization; manufacturing tolerances; performance levels; preliminary design; cold-expanded bushing.

Nomenclature

A_1	elongation rate of bushing material
A_2	elongation rate of part material
σ_{r1}	radial stress on bushing
σ_{r2}	radial stress on part
$\sigma_{r,R}$	residual radial stress
$\sigma_{\theta 1}$	circumferential stress on bushing
$\sigma_{\theta 2}$	circumferential stress on part
$\sigma_{\theta,R}$	residual circumferential stress
$\tau_{m/1}$	expansion rate applied by the mandrel to the bushing
τ_{PE}	part's maximal proportion of plastic deformation
f	static friction coefficient
F	maximum force of the actuator that pulls the mandrel through the bushing

h	bushing and part height
j	initial bushing-part clearance (for step 2)
j_m	minimum initial bushing-part clearance (for step 3)
j_M	maximum initial bushing-part clearance (for step 3)
obj_{2a}	first objective function for step 2
obj_{2b}	second objective function for step 2
obj_3	single objective function for step 3
r_{i1}	bushing inner radius
$r_{i1,R}$	residual bushing inner radius (constraint 6)
r_{i2}	part inner radius
r_{e1}	bushing outer radius
r_{e2}	part outer radius
r_{em}	mandrel external radius interfering with bushing
r_m	mandrel external radius non interfering with bushing
r_{ream}	reaming radius
r_{Y2}	yield radius of part
t_1	radial thickness of the bushing
u_C	displacement when expanding
u_R	residual displacement
X_2	vector of optimization variables for step 2
X_3	vector of optimization variables for step 3

superscripts

l	lower bound from the specifications
u	upper bound from the specifications

1 Introduction.

Optimization techniques are often employed to assist designers in the preliminary design stage [1, 2]. However, optimal designs obtained in this way are generally highly sensitive to the variability of the design parameters [3]. The field of robust design tends to take the sensitivity of the design performance into account. Robust approaches have been applied to coupled problems, like computational fluid dynamics (CFD) or fluid–structure interaction (FSI) [4]. They have also been applied to a large class of preliminary design problems, e.g. for space vehicles [5]. A comprehensive survey of robust optimization has been made by Beyer and Sendhoff [6], paying particular attention to Taguchi's robust design methodology [7]. This approach can be decomposed into three main steps: systems design, parameter design and tolerance design. The first step (systems design) is to model the problem. The parameter design step optimizes the design in order to meet the best quality requirements. Then, in the tolerance step, the design parameters are fine tuned around the optimal value in order to achieve a robust optimal design.

In Taguchi's approach, the variability is considered as an input of the problem. The goal is to find a design with steady performance. The approach that is proposed in this paper is different: it consists of finding the design that offers the maximum allowable tolerance on design variables for a given minimum performance level. This approach is very interesting for

designers as, for example, it enables a design to be found that can be manufactured at least cost while respecting the requirements. Avoiding overquality, reducing costs and increasing production rates are key issues for aerospace engineers. Usually, tolerance design is a trade-off between quality loss and manufacturing costs, which can be managed using a fuzzy quality loss function [8]. Tolerance design and process capability control can also be exploited to achieve optimum tolerance under existing capability limitations [9]. Moreover, tolerances can also be allocated by using a knowledge-based statistical approach [10].

The original trial of the approach presented here concerned modifying the third step of Taguchi's methodology. At this step, an adaptation of the initial optimization problem, used in the second step, is proposed in order to find the design that offers the maximum tolerance of the design variables while guaranteeing a minimum required level of performance. In this paper, only dimensional tolerances are considered. Note that work that manages not only dimensional tolerances but also geometric tolerances, such as parallelism, has been proposed by Hu [11].

In our approach, the previous objective functions exploited in the second step (parameter design step) are transformed into constraints at the third step. This technique, based on modifying the potential objective functions, has proved to be efficient in the preliminary design stage for the optimization of Belleville and helical springs [12-16]. Moreover, this strategy has been exploited in the optimization module of the software distributed by the Institute of Spring Technology [17]. We thus propose to exploit this method to define a new

optimization problem where the required performance level is defined by setting bounds on each performance criterion and where the objective function is to maximize the tolerances.

From a global point of view, maximizing tolerances leads to a multiobjective optimization problem. In this context, it is clear that the bounds set for each performance criterion have a major impact on the final result. Fortunately, the initial optimization procedure (defined at step two) can greatly help designers to have an overview of their design and set appropriate bounds, by calculating the maximal value of each performance criterion. Depending on the case studied, the robust optimization phase can also be associated with a graphical study that enables the designer to visualize the solution domain and choose the best design.

In order to illustrate our approach, the proposed method is applied, throughout this paper, to a highly technical application: the design optimization of a cold expanded bushing. The paper is structured as follows. Section 2 gives details of the cold expansion process itself. Then section 3 describes how the several steps of our methodology are applied to this case study. Finally, an example is given in section 4.

2. Cold-expanded bushing process

Aeronautical structures result from the assembly of numerous numerical parts. A very large number of holes are made in the components to allow the installation of fasteners. Unfortunately, it appears that such geometrical discontinuities can be critical areas [18, 19] where crack initiation can occur due to stress concentration [20]. To enhance reliability and improve the fatigue life of a given bore, a common technique is to prestress the material. For

example, the cold expansion process [21-23] consists of passing a mandrel through the bore under consideration. The mandrel is chosen to have a larger diameter than the bore, so that it expands the bore diameter to induce plastic deformation in the part. Once the mandrel is extracted, a residual compressive stress is obtained all around the bore, which tends to enhance fatigue life. In this paper, we focus on another technique that exploits the properties of materials. It consists of shrinking a bushing in a hole in order to obtain its cold expansion. This not only moderates the in-service stress concentration around the structure's hole but can be employed to avoid wear or corrosion or to repair cracked elements [19].

Figure 1 illustrates the coldworking of a clear fit bushing in the receiving part. A mandrel is force driven through the future assembly. The obtention of an interference fit is completely dependent on the values of the initial clearance between the bushing and the part, the expansion rate between the mandrel and the bushing, and the properties of the materials. The inner area of the receiving part is expected to harden as the process leads to a compressive residual stress state all around the hole.

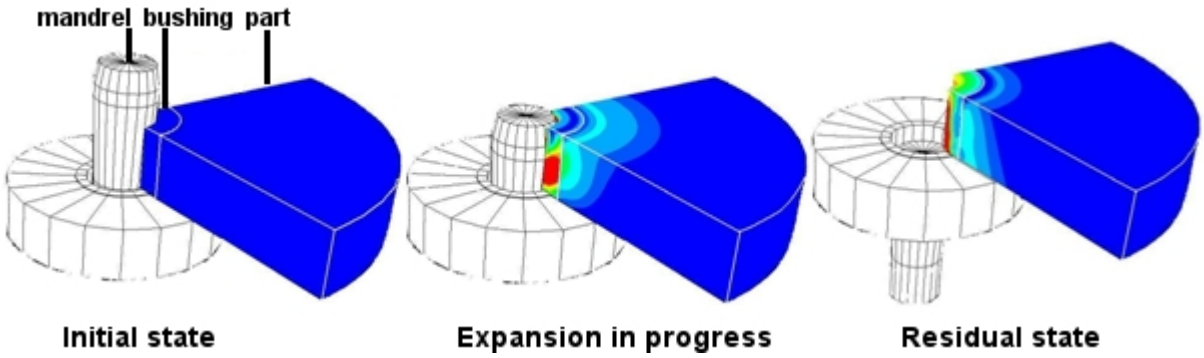

Figure 1 FE simulation of the bushing assembly by coldworking – Von Mises stress

Previous works have focused on the best combination of autofrettage and shrink-fit [24] and on the optimal cold expansion rate [25, 26]. In order to assist the designer in choosing the best process parameters, this paper deals with a question which does not seem to have been discussed in the literature: taking the geometric parameters of the problem into account, what are the optimal dimensions of the bushing and how should manufacturing tolerances be managed?

Sources of variability are multiple, e.g. manufacturing tolerances or fluctuations in material properties. In the case of aeronautical applications, material properties are very well understood. They induce a low level of variability. In contrast, the manufacturing tolerances remain unavoidable constraints. As the use of high precision machinery is expensive, obtaining a design less sensitive to manufacturing tolerances would enable costs to be reduced. In this application, the variability is thus considered as dealing with the manufacturing tolerances of the geometric parameters of the design.

Managing the diameter tolerances induces a potential clearance between the bushing and the part that must be taken into account. This is a key issue as only a simplified model with no initial clearance has been considered in previous studies in this area [24-26]. Moreover, one of the main aims of this assembly process is to guarantee the final interference fit for various geometrical data. To deal with these matters, the present work is based on a patented method described in [27]. It is implemented with a specific semi-analytical analysis of the elasto-plastic boundary problem of thick cylinders with an initial clearance. This analysis is a robust plain strain solution for the residual stresses in a cold-worked hollow cylinder derived from deformation theory [28] combined with Tresca's yield criterion. Linear work hardening behaviour is assumed for both the displacement driven expansion and the unloading step. The latter allows a constant Bauschinger effect to take advantage of the load history. This assumption is of significant importance when we are interested in the residual stress state [29, 30] and in design issues of expanded compound cylinders [31]. The Bauschinger model defined in [32] is implemented.

3. Proposed design methodology applied to the study of a cold-expanded bushing

3.1 Step 1: System design

To be correctly studied, the process first needs to be accurately modelled.

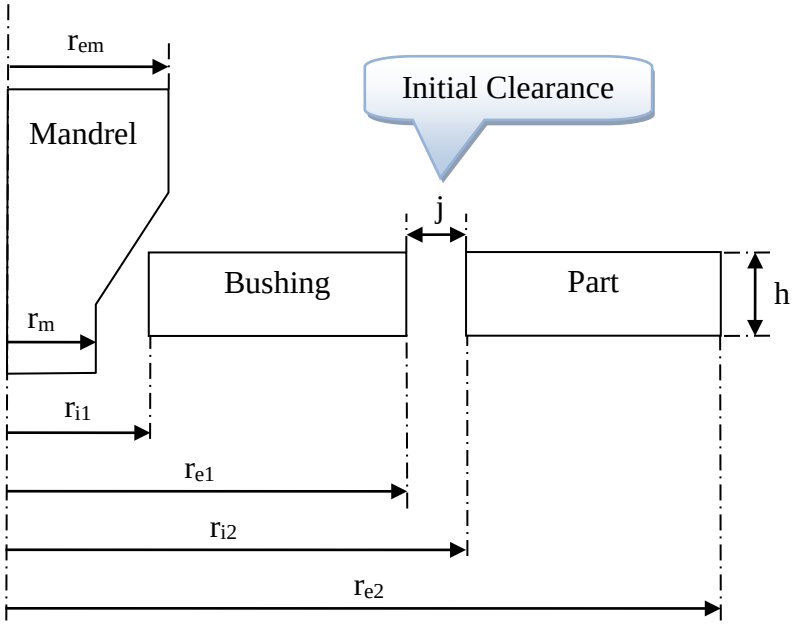

Figure 2 Axisymmetric model of the cold expanded bushing

The design parameters are described in Figure 2 and the notation is taken from [6]. The cold-expansion process operates a mandrel, e.g. through a clear fitted bushing. Both the bushing and the receiving structure are assumed to be cylindrical. We can see in Figure 2 that a potential initial clearance between the bushing and the receiving part is always considered.

3.2 Step 2: Parameter design – initial optimization problems

The parameter design step is intended to find the design that achieves the best performance. From a global point of view, several performance criteria can be considered simultaneously. To illustrate our approach, two performance criteria related to the material behaviour are

taken into account and Step 2 consists of finding the best value that can be achieved for each criterion independently. In our case, the design performance is dependent on the material behaviour. The numerous works studying the impact of coldworking on fatigue life enhancement, e.g. [21, 33], are based on a knowledge of the residual stress state. The compressive hoop stress in the part inner radius prevents crack initiation and reduces crack growth [34]. Also, the more compressive radial stress there is at the bushing/part contact, the harder it is to remove the cold expanded bushing. As compressive states are considered, the stresses are to be reduced. Thus, two objective functions can be considered:

$Obj_{2a} = \sigma_{r,R}\ (r_{i2})$: The fatigue behaviour of the receiving structure can be optimized by minimizing the residual orthoradial (hoop) stress at the part inner radius.

$Obj_{2b} = \sigma_{\theta,R}\ (r_{i2})$: The static force holding the bushing inside the part can be optimized by minimizing the residual radial stress at the bushing/part contact radius.

Thus, for a given problem, step 2 finds the optimal values of each individual objective function in order to evaluate the maximum level of performance that can be achieved for each criterion. In our study, a first optimization process minimizes the residual orthoradial stress at the part inner radius. Secondly, another optimization is performed to minimize the residual radial stress at the bushing/part contact radius. Both optimization problems exploit the same variables (see Table 1) and the same constraints (see Table 2), which are described below.

The process under study requires the implementation of various tools, such as puller units, drills, reamers, gauges and mandrels [35] to carry out the cold expansion. Having to supply a new tool set for each assembly would be too expensive. Thus, tools were selected from existing series and their characteristics were used as input data and constraints in the optimization problem. Material data were also input constants of the optimization problem.

Finally, three optimization variables referred to as vector X_2 are considered: the applied expansion rate, the initial bushing-part clearance and the inner diameter of the part (Table 1). These three geometrical variables allow the optimal design of the bushing and of the receiving diameter to be defined.

$X_2 = [\tau_{m/1}; r_{i2}; j]$	$\tau_{m/1} = \frac{r_{em} - r_{i1}}{r_{em}}$	Mandrel to bushing expansion rate
	r_{i2}	Part inner radius
	j	initial bushing-part clearance

Table 1 Optimization variables

The radius r_{em} being known, the value of the expansion rate $\tau_{m/1}$ leads to the value of r_{i1}. In a similar way, r_{i2} and j allow r_{e1} to be obtained. The constraint functions are related to the tooling, the material and the geometrical issues of the problem. As the elastic and the elasto-plastic solutions are continuous, non-assembly situations are the main challenge to be dealt with. Discontinuity in the analysis may come from a poor selection of materials or

dimensions. Sometimes the bushing never touches the part (e.g. when the clearance is too large) but non-assembly can also occur during the unloading step (e.g. the bushing does not harden enough). The constraints presented in Table 2 may be classified in two categories:

- physical limits of the problem: actuator maximum pulling power (constraint 1), mandrel path through bushing (constraint 2), minimum thickness of the bushing (constraint 3);
- design requirements: limiting the material deformation (constraints 4 and 5), reaming radius (constraint 6), maximum receiving part plastification (constraint 7), residual external radius of the part (constraint 8). Apart from the risk of cracking the parts, the material deformation can be controlled when using materials that are corrosion sensitive to stress. The residual external radius of the part is also very important as cold expansion is often used to repair existing structures on which it is not possible to modify all the dimensions.

Constraint 1	$\frac{2 \cdot \pi \cdot r_{i2} \cdot h \cdot f \cdot \sigma_{r,R}(r_{i2}) + F}{F} \leq 0$	Constraint 2	$\frac{r_m - r_{i1}}{r_m} \leq 0$
Constraint 3	$\frac{t_1^l - (r_{i2} - j - r_{i1})}{t_1^l} \leq 0$	Constraint 4	$\frac{\frac{2 \cdot u_C(r_{i1})}{\sqrt{3} \cdot r_{i1}} - A_1}{A_1} \leq 0$
Constraint 5	$\frac{\frac{2 \cdot u_C(r_{i2})}{\sqrt{3} \cdot r_{i2}} - A_2}{A_2} \leq 0$	Constraint 6	$\frac{r_{i1} + u_R(r_{i1}) - r_{ream}}{j^l} \leq 0$

Constraint 7	$\frac{\tau_{PE} \cdot (r_{e2} - r_{i2}) - (r_{e2} - r_{Y2})}{r_{e2}} \leq 0$	Constraint 8	$\frac{-r_{e2}^{u} + r_{e2} + u_R(r_{e2})}{r_{e2}} \leq 0$

Table 2 Optimization constraints

Step 2 thus consists of solving the following optimization problems:

- Minimize $obj_{2a}(X_2)$ satisfying Constraints 1 to 8
- Minimize $obj_{2b}(X_2)$ satisfying Constraints 1 to 8

The algorithms and the models are implemented in Matlab. Nested in the Optimization Toolbox, the *fmincon()* function is chosen for the optimization procedure. This function has been proved to be able to manage medium scale constrained optimization problems properly [36]. A BFGS [37-40] estimate of the Hessian and a Quadratic Programming sub-problem are solved at each iteration: the numerical solver computes the minimum value of the constrained non-linear multivariable function through Sequential Quadratic Programming [41, 42]. Involving three optimization variables, height constraint functions and out-of-reach Hessians, the problem presented here comes within the abilities of the nested optimization.

As the selected optimization procedure is a direct method based on a gradient research inside the exploration field, it is more likely to converge quickly towards the optimum if the starting point is close to the area of the solution. For that reason, when the designer does not have an initial design to suggest, the starting point is automatically chosen amongst nine potential designs, which are defined to cover the searching space as proposed by Paredes [43].

3.3 Step 3: Tolerance design – extended optimization problem with performance levels

3.3.1 How to manage tolerances on diameters

In our study, the tolerances on the two interfaces will have a major impact on the design and thus have to be considered. They depend on the four design parameters illustrated in Figure 3. The four tolerances induce a minimum and maximum value for both the expansion interference (between the bushing and the mandrel) and the initial clearance (between the bushing and the part).

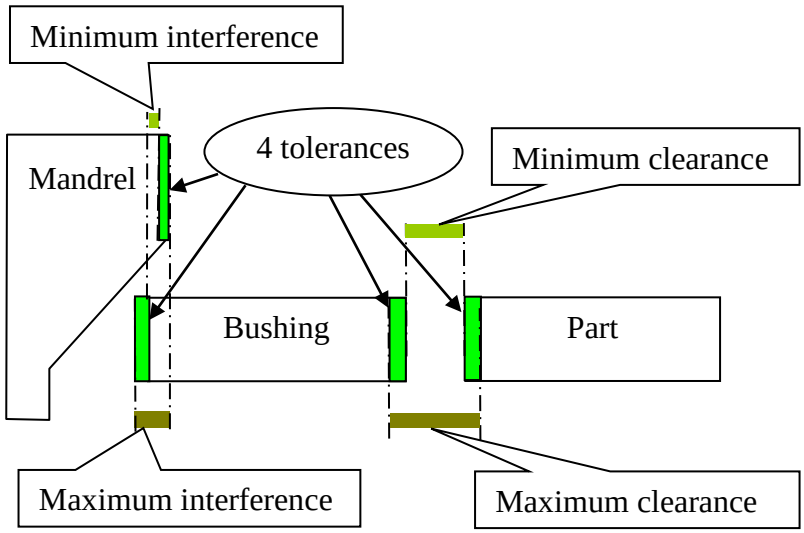

Figure 3 Design tolerances on the initial model

This problem can be transformed so as to manage only two tolerances while leading to the same range of values for the interference and the clearance:

- ✓ Tolerances on the external radius of the mandrel and the internal radius of the bushing can be merged to define the tolerance on the expansion rate and consider perfect mandrel geometry.
- ✓ Tolerances on the external radius of the bushing and on the internal radius of the part can be merged to calculate the tolerance on the initial bushing-part clearance and consider perfect receiving part geometry.

This leads to the simplified model considered in our extended optimization process, which is illustrated in Figure 4.

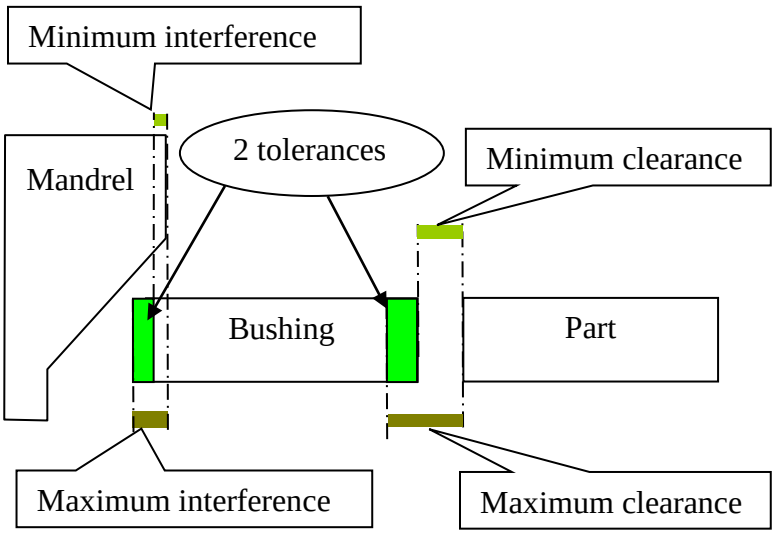

Figure 4 Design tolerances exploited by the extended optimization process

The tolerance design process is divided into two subsidiary steps to illustrate all the steps of our methodology.

Firstly, a new optimization problem is defined in order to find the inner diameter of the part that enables the maximum clearance between the bushing and the part (with no variability on the interference level). In this case, a single objective optimization is considered.

Secondly, once the inner diameter of the part is fixed, a graphical study enables the two tolerances (on the interference level and on the initial clearance) to be managed simultaneously.

3.3.2 Extended optimization process

In order to consider the range of the initial bushing-part clearance, the optimization problem is modified. Variable j, which defines the initial bushing-part clearance, is replaced by two variables, one for each bound of the domain allowable for j. Thus j_m and j_M are considered in the vector of optimization variables X_3. $j_M - j_m$ represents the allowable tolerance on the initial bushing-part clearance (Table 3).

$X_3 = \left[\tau_{m/1}; r_{i2}; j_m; j_M\right]$	$\tau_{m/1} = \frac{r_m - r_{i1}}{r_m}$	Mandrel to bushing expansion rate
	r_{i2}	Part inner radius
	j_m	Minimum initial bushing-part clearance
	j_M	Maximum initial bushing-part clearance

Table 3 Variables for the extended optimization

The new objective function is thus to find the maximum allowable tolerance i.e. the maximum value of $obj_3 = j_M - j_m$.

In that case, two designs have to simultaneously respect all the constraints: the design corresponding to the minimum value of j and the one corresponding to the maximum value of j. Thus, two elementary designs have to be considered simultaneously (see Figure 5) and the number of constraints is doubled.

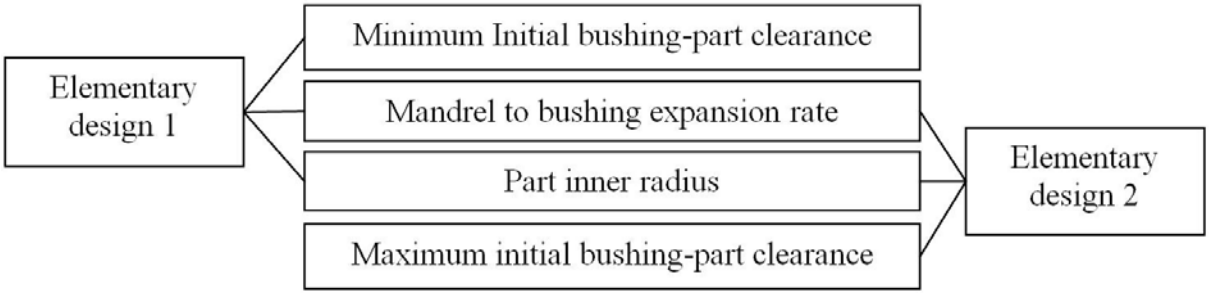

Figure 5 Details of the elementary designs considered in the extended optimization process

Moreover, as explained above, a minimum performance level now has to be guaranteed on each performance criterion. To do this, two constraints are associated with each objective function of step 2: bound constraints 9 and 10 related to $obj_{2a} = \sigma_{\theta,R}(r_{i2})$ (see Table 4), and bound constraints 11 and 12 related to $obj_{2b} = \sigma_{r,R}(r_{i2})$ (see Table 4).

Constraint 9	$\frac{\sigma^{u}_{\theta,R}(r_{i2}) - \sigma_{\theta,R}(r_{i2})}{\sigma_{\theta,R}(r_{i2})} \leq 0$	Constraint 10	$\frac{\sigma_{\theta,R}(r_{i2}) - \sigma^{l}_{\theta,R}(r_{i2})}{\sigma_{\theta,R}(r_{i2})} \leq 0$

Constraint 11	$\frac{\sigma^{u}_{r,R}(r_{i2}) - \sigma_{r,R}(r_{i2})}{\sigma_{r,R}(r_{i2})} \leq 0$	Constraint 12	$\frac{\sigma_{r,R}(r_{i2}) - \sigma^{l}_{r,R}(r_{i2})}{\sigma_{r,R}(r_{i2})} \leq 0$

Table 4 Other optimization constraints

The extended optimization problem finally considers 4 variables and 24 constraints.

- Maximize $obj_3(X_3)$ satisfying 24 constraints

Although it is bigger, the extended optimization problem is similar to the one of Step 2 and the same resolution process is exploited.

In this case study, the bounds appear in the main user interface presented in Figure 6.

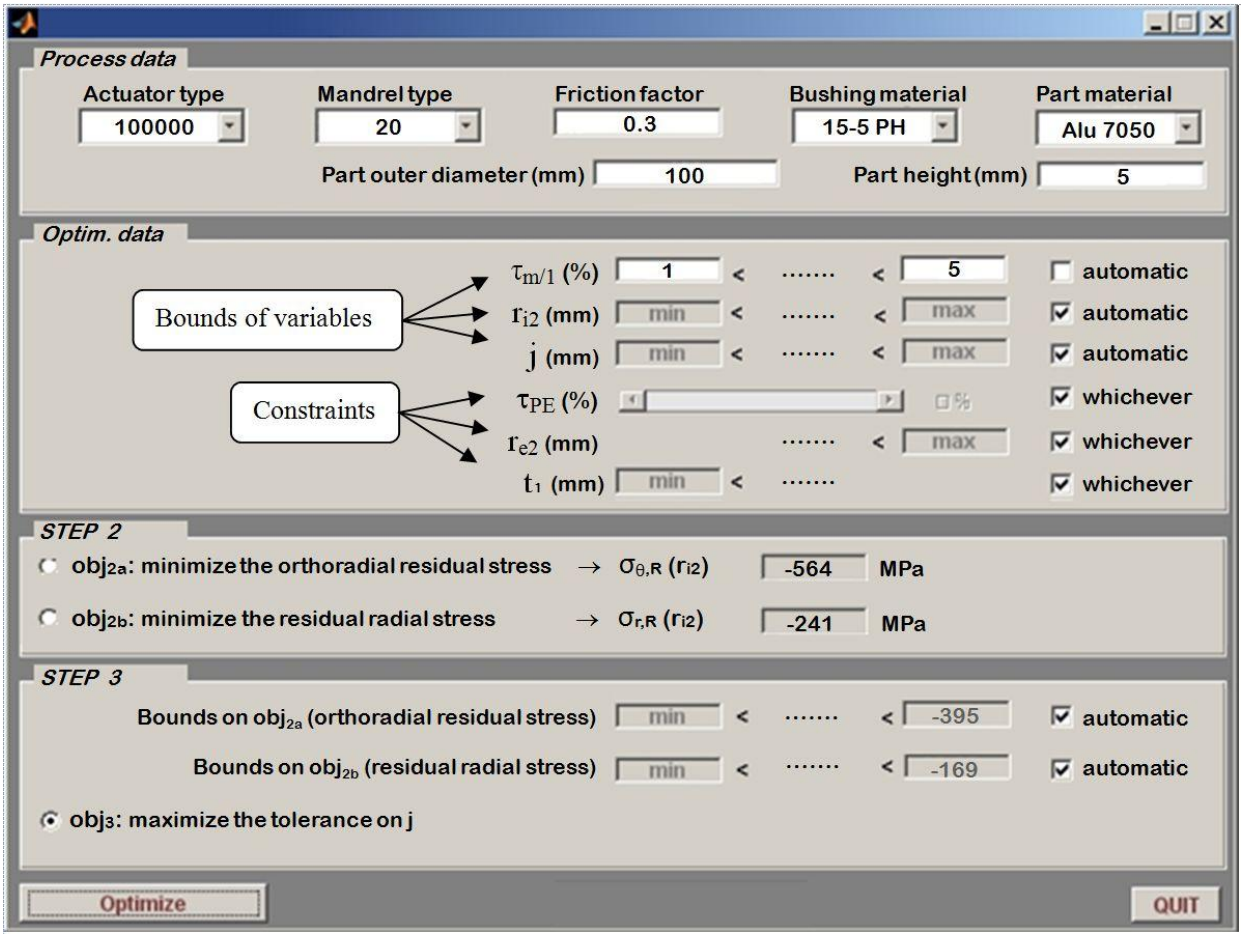

Figure 6 Main interface

Using this approach, a designer fills in all the data through the main interface, presented in Figure 6. He just has to fill in the known constraints and leave the unknown constraints for automatic definition ("automatic" and "whichever" checkboxes of Figure 6). The resolution process is designed to solve the optimization problem even if the user has not defined all its boundaries. The automatic constraints are not very tight. Thanks to this management, the

proposed geometrical optimum may point out designs that are new to the user. This exploratory approach for a better understanding of the cold expansion assembly process would not be possible if the user had to define the optimization problem entirely at each run.

The minimum performance level required clearly has a major impact on the final result. The designer can thus choose to keep an overview of the process and give the allowable bounds of both the residual orthoradial stress and the residual radial stress directly. To help the designer, the initial optimization process can be exploited to explore the design space and evaluate the allowable bounds for his problem. The whole process can also be automated by validating the checkboxes related to the residual orthoradial stress and the residual radial stress and by selecting to directly maximize the bushing-part clearance.

3.3.3 Graphical study

A further step to help designers is to provide a graphical study. The idea is to enable the solution domain to be visualized in order to highlight the mutual influence of several sources of variability. Two-dimensional visualization can be performed easily. The graphical study is thus limited to two sources of variability as managing 3 or more tolerances would be very difficult. Nevertheless, we think that the proposed approach can be useful for designers.

In the study presented, the variability considered comes from two tolerances.

We propose to select the tolerance on the bushing internal diameter as the x axis and the tolerance on the bushing/part clearance as the y axis (see Figure 7). The z axis is considered

as the nominal value of the inner diameter of the part. The graphical study thus shows the solution domain in the xy plane for a given value of z. The robust optimization step presented previously is of key interest here as it helps to select an interesting z value. The new optimization problem enables us to find the nominal value of the inner diameter of the part that offers the greatest value for the tolerance on the bushing/part clearance.

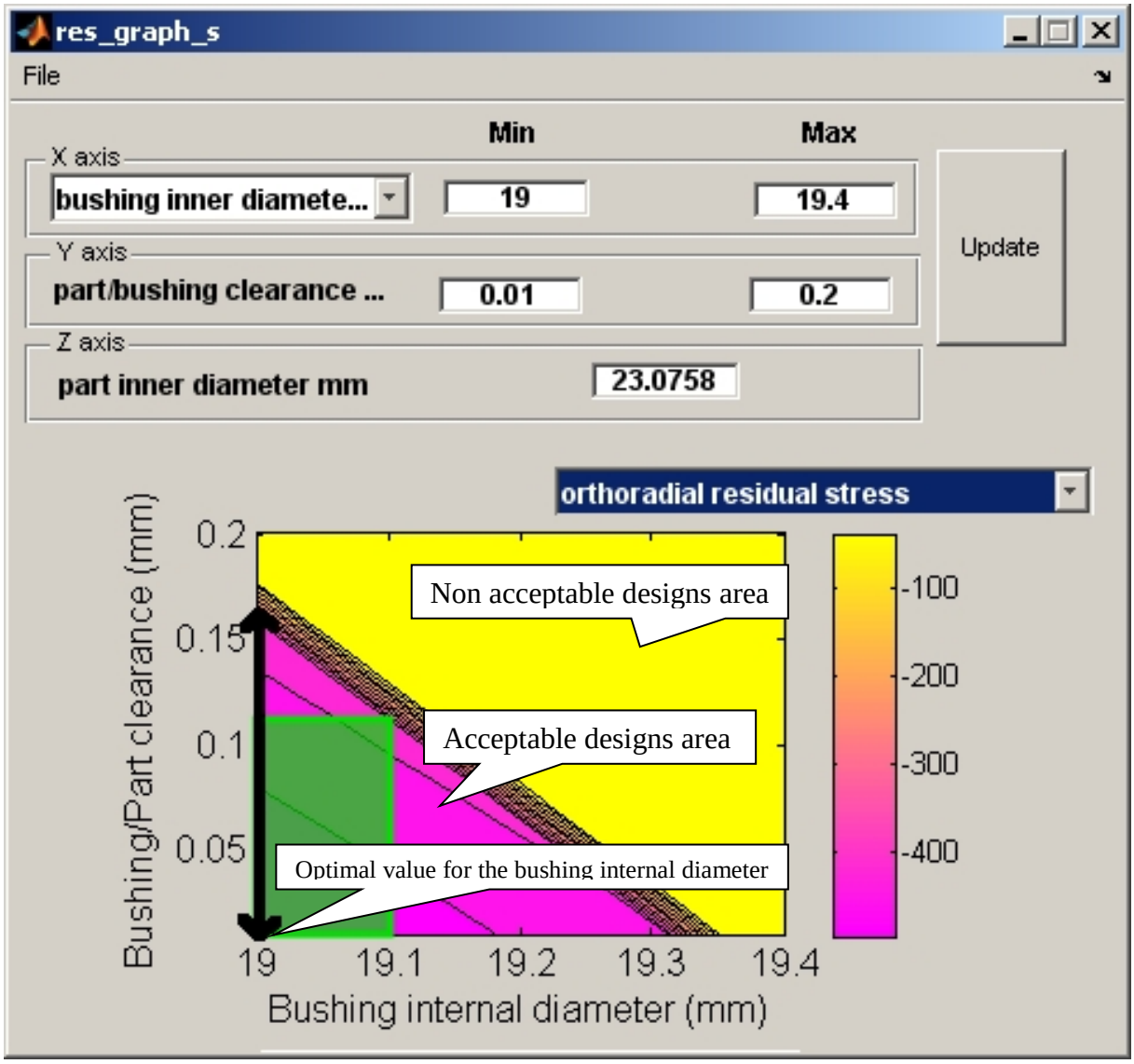

Figure 7 Graphical study to manage two tolerances simultaneously

The domain under consideration is screened regularly (10x10 = 100 points). When a point satisfies all the requirements, it is associated with the corresponding value of a selected performance criterion. When a point is out of the solution domain, a default value of 0 is

given. This enables the solution domain to be easily visualized and the value of the selected performance criterion to be appreciated.

4. Example

4.1Initial data

On a known industrial basis, the following data are chosen:

- actuator maximum pulling type: “100000” (this data leads to a pulling force = 100000 N);
- mandrel type: “20” (this data leads to a mandrel diameter = 20 mm);
- friction factor = 0.3;
- part outer diameter = 100 mm;
- part height 5 mm;
- interference rate has to stay between 1% and 5%

The mechanical characteristics of the isotropic model of the materials used are those of an AISI S15500 stainless steel for the bushing and those of a 7050-T73510 aluminium alloy for the receiving part.

4.2 Step 2: Parameter design – initial optimization problems

An optimization calculation can be started for each performance criterion (see Figure 6). The starting point is built automatically. The first process related to the minimization of the orthoradial stress leads to a minimum of -564 MPa and the second one related to the radial stress to a minimum of -241 MPa.

4.3 Step3: Tolerance optimization step

In the algorithm implemented, a 30% increase on each performance criterion is considered when the “automatic” mode is selected (see Figure 6). It leads to a limit of -395 MPa being considered on the orthoradial stress and an upper bound of -169 MPa for the radial stress. After running the “Step 3” optimization process, a resulting design that allows a 0.156 mm tolerance on the initial bushing-part clearance is proposed (see Table 5).

$X_3 = [\tau_{m/1}; r_{i2}; j_m; j_M]$	$\tau_{m/1} = 5\%$
	r_{i2} =11.538 mm
	j_m = 0.010 mm
	j_M = 0.166 mm

Table 5 Optimal design after extended optimization

At the optimal point, the active constraints are: the upper bound of $\tau_{m/1}$, the lower bound of j, the upper bound of obj_{2a} and the upper bound of obj_{2b}, which makes sense.

4.4 Graphical study step

Once the design that maximizes the tolerance on the bushing-part clearance has been found, another functionality can be exploited in order to consider the tolerance on the interference rate (e.g. the tolerance on the inner diameter of the bushing and on the external diameter of the mandrel). This consists of running the graphical study.

The new window offers a visual representation of the design space (Figure 7). The orthoradial residual stress value is given as a function of both the bushing internal diameter (x axis) and the bushing-part clearance (y axis) for a given value of the inner diameter of the part (z axis), which is set by default to the value obtained at the robust optimization step. The area where the stress is equal to 0 shows non-acceptable designs. Thus the bold black vertical arrow in Figure 7 shows the optimal design obtained when considering no tolerance on the bushing internal diameter. It is the optimal result of the previous step. Considering the two tolerances simultaneously results in a rectangle that stays inside the valid domain. For example, if a 0.1-mm tolerance is considered for the bushing internal diameter, then a maximum 0.12-mm tolerance can be accepted on the bushing-part clearance as illustrated in Figure 7. The designer can thus easily distribute the acceptable tolerance ranges over the design parameters in order to reduce production costs or increase production rates.

5. Conclusion

A robust tolerance-optimization process has been presented. The robust design methodology proposed by Taguchi searches for a steady design for a given variability defined as input. The idea developed here is to define a required performance level and then find a design that enables the allowable variability on the design parameters to be enlarged in order to reduce production costs and increase production rates. The third step of Taguchi's methodology, dedicated to tolerance management, is thus modified. Bounds are given to each performance criterion and are added as constraints in the new optimization problem, where the objective is

to maximize the variability. A graphical study that enables designers to evaluate the mutual influence of two sources of variability is also presented.

This approach is applied to the design of cold-worked bushings, which are of great interest to enhance the fatigue life of aeronautical structures and assemblies.

The present study has expanded the field of use of the cold-worked process by showing the great importance of taking the initial clearance between the part and the bushing into account as a design variable. An example that takes the industrial constraints into consideration and finds the best geometric tolerances has been presented. The sizing synthesis side of the proposed methodology could be broadened through the implementation of the material tolerances in order to study their impact on the residual state of the assembly.

References

1 Budinger M, Liscouët J et al. Estimation models for the preliminary design of electromechanical actuators. *Proc Inst Mech Eng [G]* 2012; 226: 243-259.

2 Taghavi-Zenouz R and M Afzali S. Preliminary design optimization of profile losses in multi-stage axial compressors based on complex method *Proc Inst Mech Eng [G]* 2008; 222: 951-961.

3 Doltsinis I. and Kang Z. Robust design of structures using optimization methods. *Comput Meth Appl Mech Eng* 2004; 193: 2221-2237.

4 Pons-Prats J, Bugeda G et al. Robust design optimization in aeronautics using stochastic analysis and evolutionary algorithms. *Proc Inst Mech Eng [G]* 2011; 225: 1131-1151.

5 Minisci E, Vasile M and Liqiang H. Robust multi-fidelity design of a micro re-entry unmanned space vehicle. *Proc Inst Mech Eng [G]* 2011; 225: 1195-1209.

6 Beyer H-G and Sendhoff B. Robust optimization - A comprehensive survey. *Comput Meth Appl Mech Eng* 2007; 196: 3190-3218.

7 Taguchi G. *Introduction to Quality Engineering*, American Supplier Institute, 1989.

8 Cao Y, Mao J et al. A robust tolerance optimization method based on fuzzy quality loss. *Proc Inst Mech Eng [C]* 2009; 223: 2647-2653.

9 Yu K-T and Shen C-Y. A Combining tolerance design and monitoring process capability in a design-manufacturing integration procedure. *Proc Inst Mech Eng [B]* 2009; 223: 1389-1394.

10 Swift K G, Raines M and Booker J D. Tolerance optimization in assembly stacks based on capable design. *Proc Inst Mech Eng [B]* 1999; 213: 677-693.

11 Hu J and Peng Y. Tolerance modelling and robust design for concurrent engineering. *Proc Inst Mech Eng [C]* 2007; 221: 455-465.

12 Paredes M and Daidie A. Optimal catalogue selection and custom design of Belleville spring arrangements. *Int J Inter Des Manuf* 2010; 4: 51-59.

13 Paredes M and Rodriguez E. Optimal design of conical Springs. *Eng Comput* 2009; 25: 147-154.

14 Paredes M, Sartor M and Daidie A. Advanced assistance tool for optimal compression spring design. *Eng Comput* 2005; 21: 140-150.

15 Paredes M, Sartor M and Masclet C. Obtaining an optimal compression spring design directly from a user specification *Proc Inst Mech Eng [B]* 2002; 216: 419-428.

16 Paredes M, Sartor M and Masclet C. An optimization process for extension spring design. *Comput Meth Appl Mech Eng* 2001; 191: 783-797.

17 Spring Calculator Professional, Institute of Spring Technology, Henry Street, Sheffield S3 7EQ, UK, http://www.springcalculator.com/scp/features.html (2013, accessed 2 January 2013)

18 Ransom J, Restis J and Weiss M. F-16 Fighting Falcon Upper Fuselage Skin Fatigue Life Enhancement. In: *USAF Aircraft Structural Intergrity Program Conference,* San Antonio, Texas, 1999.

19 Mann JY et al. The Use of Interference-Fit Bolts or Bushes and Hole Cold Expansion for Increasing the Fatigue Life of Thick-Section Aluminium Alloy Bolted Joints. Report for the defense science and technology organisation aeronautical research loboratories, Melbourne, Victoria, Report no. AD-A142 083, 1983.

20 Robinson P A, Swift K G et al. An expert system for the determination of stress concentration factors. *Proc Inst Mech Eng [G]* 2001; 215: 219-228.

21 Gaerke J, Zhang X and Wang Z. Life enhancement of fatigue-aged fastener holes using the cold expansion process. *Proc Inst Mech Eng [G]* 2000; 214: 281-293.

22 Mahendra Babu NC et al. A simplified 3-D finite element simulation of cold expansion of a circular hole to capture through thickness variation of residual stresses. *Eng Fail Anal* 2008; 15: 339–348.

23 Gopalakrishna HD et al. Cold expansion of holes and resulting fatigue life enhancement and residual stresses in Al 2024 T3 alloy – An experimental study. *Eng Fail Anal* 2010; 17: 361–368.

24 Jahed H, Farshi B and Karimi M. Optimum Autofrettage and Shrink-Fit Combination in Multi-Layer Cylinders. *J Press Vessel Technol* 2006; 128: 196-200.

25 Amrouche A et al. Numerical study of the optimum degree of cold expansion: Application for the pre-cracked specimen with the expanded hole at the crack tip. *J Mat Proces Technol* 2008; 197: 250.

26 Giglio M, M. Lodi. Optimization of a cold-working process for increasing fatigue life, Int J Fat 31 2009; 1978:1995.

27 Canivenc R, Sartor M et al. *Method, system and computer program product for calculating the residual stress equilibrium of two concentric cylinders coldworked by a loading-unloading expansion process*. Patent, USA, 2007.

28 Hencky H. Zur Theorie Plastischer Deformationen und der Hierdurch im Material Hervorgerufenen Nachspannungen. In: 1st *International Congress on Applied Mechanics*, Delft,1924.

29 Chen P.C.T. Bauschinger and hardening effect on residual stresses in an autofrettaged thick-walled cylinder. *J Press Vessel Technol* 1986; 108: 108-112.

30 Levy C, Perl M and Kotagiri S. The Bauschinger effect's influence on the SIFs of multiple longitudinal coplanar cracks in autofrettaged pressurized cylinders. *Eng Frac Mech* 2006; 73: 1814.

31 Parker AP. Bauschinger Effect Design Procedures for Compound Tubes Containing an Autofrettaged Layer. *J Press Vessel Technol* 2001; 123: 203-206.

32 Ball DL. Elastic-plastic stress analysis of cold expanded fastener holes. *Fat fract eng mat struct* 1995; 18: 47-63.

33 Duprat D et al. Fatigue life prediction of interference fit fastener and cold worked hole. *Int J Fat* 1996; 18: 515-521.

34 Withers PJ and Bhadeshia H K D H. Residual Stress Part 2 - Nature and origins. *Mat Sci Technol* 2001; 17: 366-375.

35 FTI, Fatigue Technology Cold Expansion System Tooling Catalogue - Revision 5. 2004, Fatigue Technology Inc.: Seattle, 2004

36 Vanderplaats GN. *Numerical optimization techniques for engineering design*. 3rd ed. Vanderplaats Research and Development, Inc. 2001.

37 Broyden CG. The Convergence of a Class of Double-rank Minimization Algorithms. *J Inst Math Appl* 1970; 6: 76-90.

38 Fletcher R. A New Approach to Variable Metric Algorithms. *Comp J* 1970; 13: 317-322.

39 Goldfarb D. A Family of Variable Metric Updates Derived by Variational Means. *Math Comput* 1970; 24: 23-26.

40 Shanno DF. Conditioning of Quasi-Newton Methods for Function Minimization. *Math Comput* 1970; 24: 647-656.

41 Powell MJD. A Fast Algorithm for Nonlinear Constrained Optimization Calculations. *Num Anal Lect not math* 1978; 630: 144-157.

42 Coleman TF and Li YY. An Interior Trust Region Approach for Nonlinear Minimization Subject to Bounds. Cornell University: Ithaca, NY, USA, 1993.

43 Paredes M. Methodology to build an assistance tool dedicated to preliminary design: application to compression springs. *Int J Inter Des Manuf* 2009; 3: 265-272.